Article

Compact Thermal Modeling of Modules Containing Multiple Power LEDs

Marcin Janicki [1,*], Przemysław Ptak [2], Tomasz Torzewicz [1] and Krzysztof Górecki [2]

[1] Department of Microelectronics and Computer Science, Lodz University of Technology, 90-924 Łódź, Poland; torzewicz@dmcs.pl
[2] Department of Marine Electronics, Gdynia Maritime University, 81-255 Gdynia, Poland; p.ptak@we.umg.edu.pl (P.P.); k.gorecki@we.am.gdynia.pl (K.G.)
* Correspondence: janicki@dmcs.pl; Tel.: +48-42-6312654

Received: 20 May 2020; Accepted: 15 June 2020; Published: 17 June 2020

Abstract: Temperature is an essential factor affecting the operation of light-emitting diodes (LEDs), which are often used in circuits containing multiple devices influencing each other. Therefore, the thermal models of such circuits should take into account not only the self-heating effects, but also the mutual thermal influences among devices. This problem is illustrated here based on the example of a module containing six LEDs forming on the substrate a hexagon. This module is supposed to operate without any heat sink in the natural convection cooling conditions, hence it has been proposed to increase the thermal pad area in order to lower the device-operating temperature. In the experimental part of the paper, the recorded diode-heating curves are processed using the network identification by deconvolution method. This allows for the computation of the thermal time constant spectra and the generation of device-compact thermal models. Moreover, the influence of the thermal pad surface area on the device temperature and the thermal coupling between LEDs is investigated.

Keywords: multi-LED lighting modules; device thermal coupling; compact thermal models

---

1. Introduction

Nowadays, light-emitting diodes (LEDs) have replaced traditional incandescent light bulbs in virtually all everyday applications, becoming the most frequently used light source [1–3]. Taking into account that their operation involves physical phenomena of different natures, such as electrical, optical or thermal ones, the modeling of these devices calls for a truly multi-domain approach [4–6]. Beyond any doubt, among the main factors influencing the performance of LEDs and affecting their parameters is temperature. Therefore, the accurate prediction of LED junction temperature is crucial for the stability of their lighting parameters and the long life of these light sources [7–11]. Thus, the design and the thermal management of luminaires containing LED light sources requires accurate thermal models [12–16]. Moreover, LED light sources are often manufactured also as modules including drivers consisting of power transistors on the same substrate, hence thermal models of these devices should accurately reflect both self- and mutual heating effects [17–24]. Unfortunately, in most cases, the detailed models of LED modules are not readily available or they have unacceptably long simulation times. Thus, these models are usually realized in a reduced SPICE-like compact form, which could be then easily included in some standard electrical or multi-domain simulators [7,25].

In this paper, the authors present a methodology to generate such compact thermal models based on the practical example of a module containing six power LEDs, which are soldered to an metal core printed circuit board (MCPCB) in the shape of a regular hexagon. This module was developed for specific customer needs and it will serve for the lighting of a worker's operating field at an assembly line, where the intensity of light will be automatically controlled depending on the available daylight [26].

In such applications, the use of multi-LED modules is beneficial because it allows a more accurate distribution of light intensity for lower currents flowing through multiple LEDs. Moreover, taking into account that, because of the limited space, this module in its end-use application is to be cooled only by the means of natural convection without any heat sink, two versions of the module, differing in the size of the thermal pads under the LED packages, were considered.

The following section of this paper introduces the prototype modules, measurement equipment and the adopted research methodology. Then, the temperature measurement results are presented in detail. The acquired experimental data allowed the computation of the thermal structure functions and time constant spectra, hence rendering possible the generation of compact thermal models, which were obtained in the form of Cauer RC ladders. These models were used for the simulations of device heating curves taking into account thermal couplings between the devices. The simulation results were validated against measurements. Finally, the Cauer ladders were converted into their Foster counterparts and their element values were analyzed, demonstrating the important influence of an increased thermal pad area on device temperature.

2. Research Methodology

2.1. Prototype Modules and Measurement Euqipment

The test modules analyzed throughout this paper contained six LEDs forming on the substrate, as presented in Figure 1a, a hexagonal circle with the diameter equal to 27 mm. The investigated white diodes of the XREWHT-L1-0000-006F8 type belonged to the XLamp® family manufactured by Cree. Their maximal forward current value is 0.7 A and their viewing angle is 90°. The dimensions of the MCPCB used for these modules were 50 mm × 50 mm × 1.5 mm. These substrates are dedicated for LED applications and according to the datasheet provided by the manufacturer, their thermal conductivity value is equal to 2 W/(m·K). In order to investigate the influence of the thermal pad area on the LED temperature, the modules were fabricated in two different versions. The first one had the standard size of diode thermal pads, i.e., equal to 6.46 mm × 5.60 mm. Their dimensions, as visible in Figure 1b, were delimited by the LED package width and the spacing between the diode electrodes. The other version of the module had the pad width doubled to 12.92 mm. These large pads are visible in Figure 1a as the light rectangles extending outside the package perimeter.

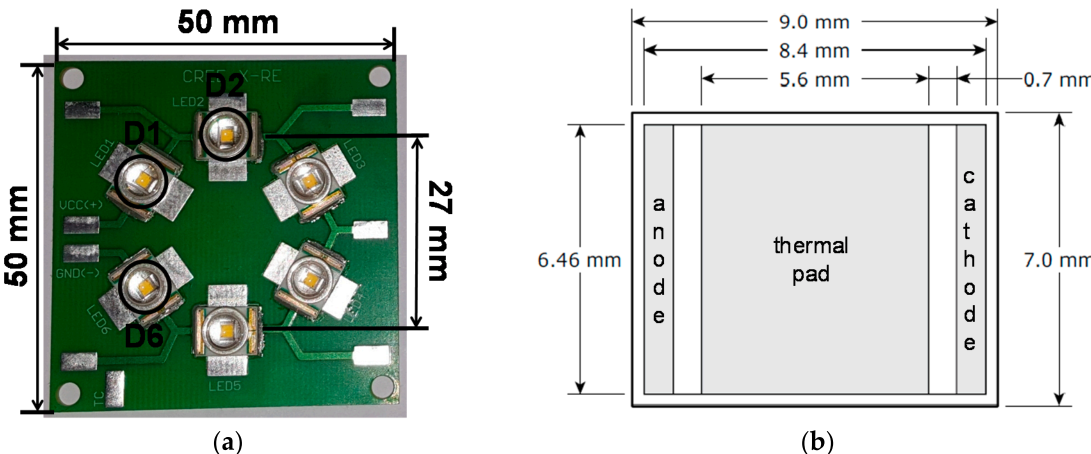

Figure 1. Dimensions of the investigated multi-, light-emitting diodes (LEDs) test module: (**a**) the photograph of the circuit layout; (**b**) the LED electrode layout at the bottom side of the package.

Taking into account the prospective application of the modules, the main goal of the research was to determine the mutual influences between the devices. Looking at the circuit layout, it could be concluded that there existed three possible distances between the devices: 14.1 mm, 24.2 mm or 27.0 mm, therefore it would be enough to include only four LEDs in the thermal coupling analyses.

Thus, the diode D2 was initially used as a heat source and the temperature values were measured in the diodes D1–2 and D5–6, but it soon turned out that the responses in the two latter devices were very similar. Hence, the analyses presented in the remainder of this paper will be limited only to the LEDs marked in Figure 1a with black circles. This solution allowed to keep the figures legible without any significant loss of the analysis depth.

The thermal couplings between the devices were investigated based on the results of dynamic temperature measurements, which were taken with the T3Ster® transient thermal tester produced by Mentor®. This piece of equipment renders possible the registration of the system's thermal responses with microsecond time resolution [27]. During the measurements, the diode cathode and anode terminals were soldered to the standard measurement cables provided together with the tester and the MCPCB was placed horizontally in thermally insulated clamps.

2.2. Theoretical Backgound

The entire research methodology employed throughout this paper can be summarized as shown in Figure 2. First, the temperature sensitivity of all LEDs has to be determined and then their thermal responses to the power step thermal excitations have to be recorded. Then, according to the principles of the network identification by deconvolution (NID) method, these responses have to be numerically differentiated so as to obtain the responses to the Dirac delta function and then the deconvolution operation produces the thermal time constant spectra [28], which after segmentation, according to the later described procedure, yield initial compact thermal model element values. Finally, these values are further optimized so as to minimize the simulation errors with respect to the measurements [29].

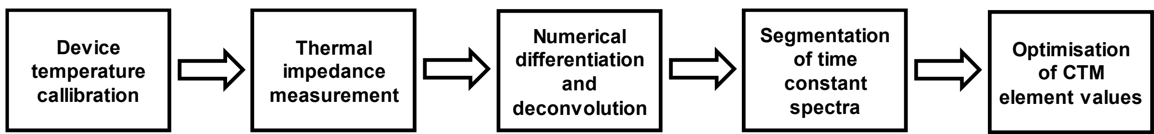

Figure 2. The flowchart illustrating the research methodology employed throughout this paper.

3. Experimental Results

3.1. Device Callibration

Before the actual measurements, each of the investigated devices was calibrated on a cold plate for the forward current of 10 mA. The measured dependencies of diode voltage on temperature are presented in Figure 3a. The black markers and lines correspond to the module having the thermal pads of standard size (STP), whereas the lighter ones to the module with double size thermal pads (DTP). As can be seen in the chart, for each diode this dependence is fairly linear but the measured sensitivity values vary, substantially falling in the range of 1.46÷2.23 mV/K. This result suggests thermal models should be developed independently for each device.

3.2. Transient Thermal Response Measuremnts

This paper will illustrate in detail how the compact thermal model was derived for the diode D2. A similar procedure should be applied for the other LEDs. Initially, during the measurements the constant current of 700 mA was forced through this diode until the thermal steady state was reached, and then, after switching it off, transient temperature responses were measured in the heating device and in the diodes D1 and D6. The measurement current was the same as during the calibration, i.e., 10 mA.

The measurement results are represented in Figure 3b as heating curves, which were obtained by subtracting the recorded diode cooling curves from the respective steady state temperature rise values. The black color in this figure denotes the module with the standard thermal pads. The solid, dashed and double lines are used for the diodes D2, D1 and D6, respectively. The forced LED heating current

value was equal to 700 mA, and the measured electrical power was 2.23 W with the standard pad, and 2.18 W with the double one.

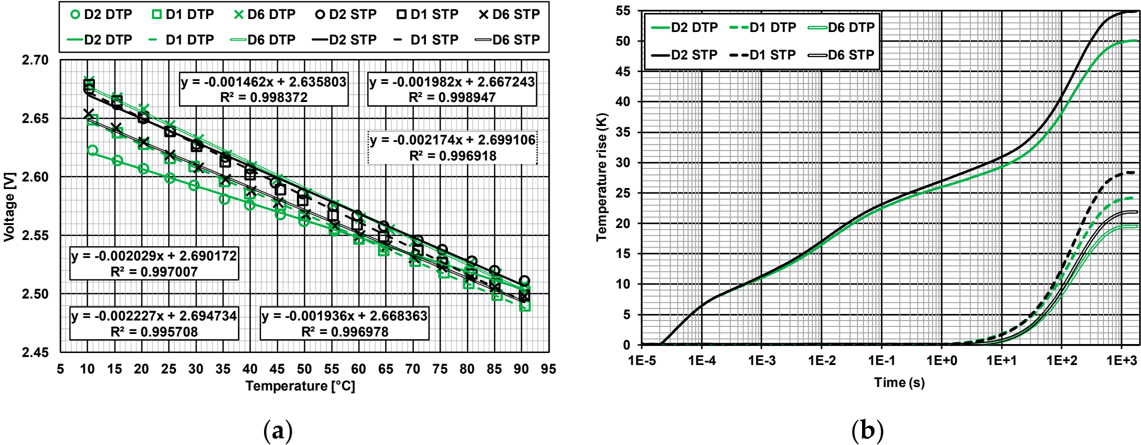

(**a**) (**b**)

Figure 3. LED measurement results: (**a**) the LED voltage temperature sensitivity; (**b**) the diode heating curves at 700 mA current.

The thermal response in the heating device, as can be seen in the figure, develops almost immediately. The heat diffuses to the other diodes already within a few seconds, reaching 10% of the final temperature rise value in remote devices after more than 20 s. Although the thermal responses in these devices are visibly attenuated, their steady state temperature rise values amount to at least 40% of the maximal temperature rise in the heating diode, hence indicating the existence of the important thermal coupling between the diodes. The measured steady state temperature values in the devices with the larger thermal pads are always at least 10% lower and the influence of the pad in the heating diode becomes visible already after 100 ms. The effect of a larger thermal pad becomes visible already when heat diffuses into the MCPCB in less than a second. This is probably due to the fact that the thermal pad works similarly as the traditional heat spreader, which facilitates the heat removal from the package.

3.3. *Computation of Thermal Structure Functions and Time Constant Spectra*

According to the JEDEC standards [30,31], all thermal analyses should be always carried out using the real heating power as the input quantity, which can be found by subtracting from the measured electrical power the value of the optical power emitted in the form of light. Thus, it was also necessary to determine the value of the LED optical power, which could be computed using the method described in [32], based on the knowledge of the measured light intensity at a known distance directly over the diode and the spatial light distribution curve provided by the manufacturer in the datasheet. For the LED heating current considered here, the measured optical and real heating power values were equal to 0.4 W and 1.8 W. Unfortunately, without the information concerning the internal diode structure, it was not possible to evaluate how much heat was dissipated in the semiconductor structure itself and how much was dissipated during the wavelength conversion in phosphorus.

Once knowing the LED heating power, the measured curves were processed using the network identification by deconvolution (NID) method offering the entire set of different thermal analysis tools [28]. The thermal cumulative structure functions and the time constant spectra computed using this method are presented in Figure 4. The cumulative thermal structure functions in Figure 4a show the entire heat flow path from the junction (the origin of the co-ordinate system) to the ambient (the steep vertical line at the end). The deflection points in these curves indicate the heat diffusion to another material, and the horizontal plateaus indicate the total accumulated thermal capacitance.

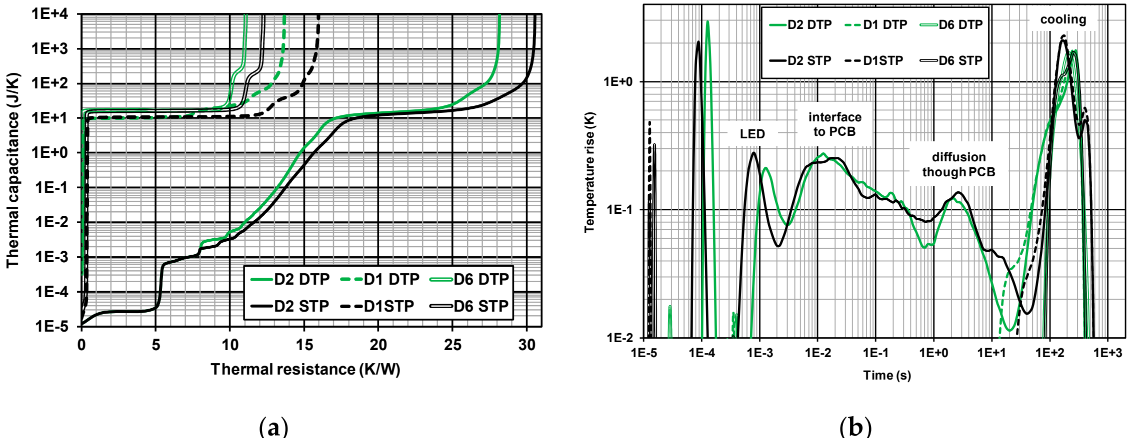

(**a**) (**b**)

Figure 4. Thermal analysis results: (**a**) the cumulative structure functions; (**b**) the time constant spectra.

Normally, the structure functions are computed only for the driving point thermal impedance, i.e., diode D2 in this case, but here we also included the curves computed for the remote diodes, which have only the large plateau corresponding to the PCB capacitance. The curves for the heating diode D2 have three distinct flat sections, which most probably correspond to the LED die, package and board capacitances. The influence of the larger thermal pad only becomes visible when heat diffuses into the substrate, i.e., for the thermal capacitance over 1 mJ/K and for a resistance of around 8 K/W. All the lighter curves at their ends are shifted visibly to the left of their black counterparts, what confirms the earlier observation that the use of a large thermal pad can effectively reduce the total thermal resistance.

The time constant spectra of the thermal responses computed using the NID method are presented in Figure 4b. In order to expose the short time constant components, the spectra presented here were initially integrated over time. As can be seen, the spectra in the figure contain large thermal time constant components related to the heat exchange with ambient, visible large peaks located around 200 s. Short-time constants are present only in the temperature responses of the heating diode. This part of the heat flow path can be analyzed by dividing the spectra into individual sections in the locations of the minima. These sections are additionally indicated in the figure by the text labels. Consequently, the low thermal resistance section from just below a second to around half a minute reflects the conduction of the heat through the MCPCB. Furthermore, the peaks with the maxima in the range of 10÷30 ms correspond to the interface between the package and the board. The remaining part of the spectra below the minima located at a couple of milliseconds describe the heat flow inside the LED package, except for the narrow peaks visible at tens of microseconds, which are just the artefacts after the removal of the electrical transients from thermal responses.

3.4. Foster RC Ladder Compact Thermal Models

For the generation of the circuit compact thermal models (CTMs), the time constant spectra for the heating LED were divided, as previously discussed, into four individual segments corresponding to the diode package, the interface to the MCPCB, the conduction through the board and the heat exchange with the ambient. This procedure yielded CTMs in the form of four stage Foster RC ladder models. In the case of other LEDs, the models had only one RC stage, which will then be used for the computation of mutual thermal couplings.

Consistent with the method described in [29], initially, the thermal resistor values in all the CTM stages were determined by separately accumulating the respective thermal resistances in each section. Then, the time constant values were found by minimizing the simulation errors with respect to the measured temperature values within each time constant range. Finally, the capacitor values were computed by dividing the respective time constant and resistor values. The heating curves obtained with these models for all the considered diodes in the case of the test module with the standard size

thermal pads are compared with the measured values in Figure 5. The lighter lines (simulated (SIM)) are used for the simulated values whereas the measured ones (MES) are represented by the black ones.

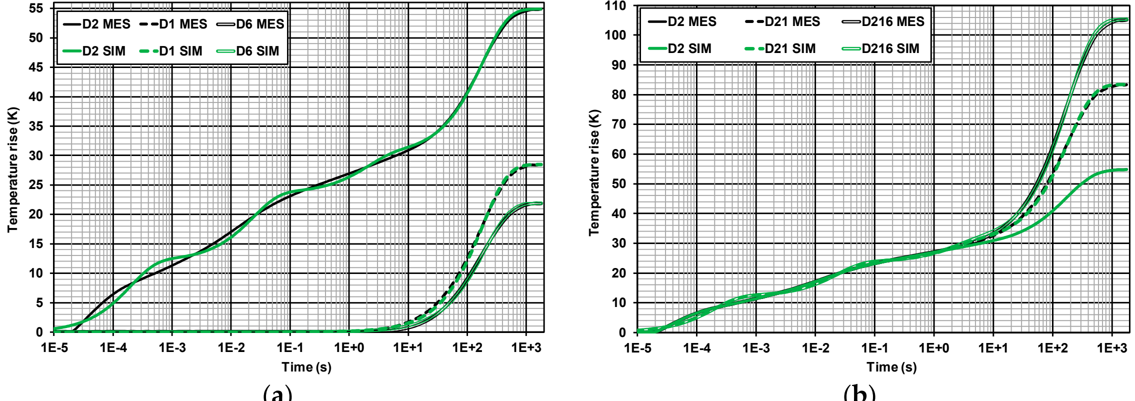

Figure 5. Comparison of measured (MES) and simulated (SIM) heating curves for the LED module with the standard size thermal pads: (**a**) in the different diode locations when only diode D2 is heating; and (**b**) in diode D2 for the different number of heating diodes.

When power was dissipated only in the diode D2, see Figure 5a, the simulation results were very accurate for the time instants over 1 s, where the errors did not exceed 0.7 K. These differences in the time range from 0.1 ms to 1 ms even reached 2.5 K, but the simulation accuracy could be further improved by dividing the first section of the CTM into more segments corresponding to the two distant peaks in the time constant spectra in this region, or by changing the method used to remove the electrical transients from the registered thermal responses. The generated CTMs were also used for simulations when the module was heated by more than one diode, i.e., diodes D2 and D1 (denoted in Figure 5b as D21), and then with the diode D6 (marked as D216) as the third heat source. As can be seen, the thermal coupling between the devices becomes visible only after a few seconds, but the two remote LEDs contribute 50 K to the overall temperature rise of diode D2, which is almost the same value as due to the self-heating.

Generally, the diode heating curves presented in Figure 5 can be generated employing the formula given in Equation (1), where the first component represents the four stage RC model of the k-th diode and the second component describes the mutual heating by neighboring devices with the one-stage CTMs. P denotes here the respective heating powers of each device:

$$T_k(t) = P_k \sum_{i=1}^{4} R_{ki}(1 - \exp(-t/\tau_{ki})) + \sum_{j=1}^{5} P_j R_j\left(1 - \exp\left(-t/\tau_j\right)\right) \tag{1}$$

3.5. Cauer Element Values

The previously presented heating curves were obtained with the Foster ladder CTMs because of the straightforward implementation of the mathematical formulas to compute thermal responses. However, as demonstrated in [33], the element values of these models cannot have any physical interpretation because they contain a chain of capacitors linking the diode junction to the ambient, which implies an immediate propagation of thermal responses through the entire module. Therefore, the CTMs were converted to the mathematically equivalent Cauer ladders, which have all their capacitors connected to the thermal ground, so their element values can have some physical interpretation. The conversion was carried out using the algorithm proposed in [34]. The CTM element values for the modules with the standard thermal pad and the doubled one are given in Tables 1 and 2 respectively.

Table 1. Cauer ladder element values for the standard thermal pad.

Device	τ (s)	Rth (K/W)	Cth (J/K)
D2	1.951×10^{-4}	6.837×10^{0}	2.853×10^{-5}
	2.326×10^{-2}	6.403×10^{0}	3.633×10^{-3}
	2.020×10^{0}	3.851×10^{0}	5.245×10^{-1}
	1.759×10^{2}	1.347×10^{1}	1.306×10^{1}
D1	1.805×10^{2}	1.597×10^{1}	1.131×10^{1}
D6	1.960×10^{2}	1.224×10^{1}	1.601×10^{1}

Table 2. Cauer ladder element values for the double thermal pad.

Device	τ (s)	Rth (K/W)	Cth (J/K)
D2	1.819×10^{-4}	6.676×10^{0}	2.725×10^{-5}
	2.090×10^{-2}	6.063×10^{0}	3.446×10^{-3}
	1.181×10^{0}	3.259×10^{0}	3.623×10^{-1}
	1.714×10^{2}	1.218×10^{1}	1.407×10^{1}
D1	1.716×10^{2}	1.366×10^{1}	1.256×10^{1}
D6	1.896×10^{2}	1.105×10^{1}	1.716×10^{1}

The largest time constants of around 3 min contribute over 40% of the thermal resistance in the heating device, and they correspond to the heat exchange with the ambient. These time constants are the only ones present in the responses of the remote diodes, and as mentioned before, the one-stage CTMs generated for these remote diodes can be used for simulations of the thermal couplings between the heating diode and other LEDs, as it was proposed for multi-chip modules in [35]. The time constant around a couple of seconds reflects the heat conduction through the MCPCB and it contributes the least portion to the total thermal resistance. The time constant of just over 20 ms models the interface between the package and the board and the thermal capacitance of this stage equal to around 3.5 mJ/K could be possibly attributed to the diode package. Finally, the shortest time constant of just below 200 µs can be associated with the semiconductor die. Then, the resistance is the junction to the solder point one, given in the datasheets (typically 8 K/W for this device), and the thermal capacitance of the die is equal to almost 30 µJ/K. This value corresponds well to the plateau in the thermal structure functions presented in Figure 4a. Comparing the tables for the standard size thermal pad and the doubled one, it is visible that the major difference arises for the time constants around a few seconds, where both the resistance and capacitance values are noticeably lower for the module with the larger thermal pads, hence confirming that the generated heat is more effectively evacuated from the package to the board.

4. Conclusions

The research results presented in this paper demonstrated the existence of important thermal couplings in the modules containing multiple LEDs and cooled by natural convection without a heat sink. In particular, it was experimentally shown that when cooling is poor the diode self-heating can contribute only a small portion to the total device junction temperature rise over the ambient. Thus, the heating by neighboring devices might become more important than the temperature rise due to the heat generated in a particular device. Therefore, the CTMs used for the simulations of such modules should take into account the mutual thermal interactions between the devices when applied cooling is poor. Obviously, this problem will not be so severe, when a proper heat sink is attached, but sometimes this might not be possible because of various design constraints. Another important contribution of this research was to demonstrate that the thermal pad area noticeably influences the junction-to-board thermal resistance.

From the theoretical point of view, this paper illustrated the methodology to derive compact thermal models when power is dissipated in multiple devices. This methodology turned out to be

effective and the thermal simulations carried out with the resulting dynamic compact models were accurate. However, it should be underlined that in the considered case, the geometry of the circuit layout was symmetrical and the circuit contained devices of the same type. Thus, in the general case, the reciprocity of mutual thermal influences would not hold. The main limitation of the proposed methodology was that the compact model element values depend on the device operating conditions and that they also vary among individual devices. Therefore, the compact models have to be derived separately for each LED. These differences result not only from different LED temperature sensitivities, but also from different LED soldering thermal resistances and other factors. Another interesting observation from the system designer point of view is that increasing the area of LED thermal pads can effectively reduce the device temperature rise already after a second. In the steady state, it was possible to lower the temperature even by 10% when only one device was active. This effect could be increased when more devices are dissipating power. In further investigations, a more in-depth study of the thermal pad area should be carried out.

Author Contributions: The measurements presented in this manuscript and their evaluation was carried out by P.P. and T.T. The research on the generation of compact models and thermal simulations was done by M.J. Finally, M.J. and K.G. supervised the research and prepared the manuscript. All authors have read and agreed to the published version of the manuscript.

Funding: This research was supported financially from the Ministry of Science and Higher Education program "Regional Excellence Initiative" 2019-2022 project No. 006/RID/2018/19, the sum of financing 11,870,000 PLN.

Conflicts of Interest: The authors declare no conflict of interest.

References

1. Weir, B. Driving the 21st century's lights. *IEEE Spectr.* **2012**, *49*, 42–47. [CrossRef]
2. Schubert, E.F. *Light Emitting Diodes*, 3rd ed.; Rensselaer Polytechnic Institute: Troy, NY, USA, 2018.
3. Lasance, C.J.M.; Poppe, A. (Eds.) *Thermal Management for LED Applications*; Springer: Dordrecht, The Netherlands, 2014.
4. Poppe, A.; Farkas, G.; Gaál, L.; Hantos, G.; Hegedüs, J.; Rencz, M. Multi-domain modelling of LEDs for supporting virtual prototyping of luminaires. *Energies* **2019**, *12*, 1909. [CrossRef]
5. Martin, G.; Marty, C.; Bornoff, R.; Poppe, A.; Onushkin, G.; Rencz, M.; Yu, J. Luminaire digital design flow with multi-domain digital twins of LEDs. *Energies* **2019**, *12*, 2389. [CrossRef]
6. Poppe, A. Simulation of LED based luminaires by using multi-domain compact models of LEDs and compact thermal models of their thermal environment. *Microelectron. Reliab.* **2017**, *72*, 65–74. [CrossRef]
7. Biber, C. LED Light Emission as A Function of Thermal Conditions. In Proceedings of the 24th IEEE Semiconductor Thermal Measurement and Management Symposium, San Jose, CA, USA, 16–20 March 2008; pp. 180–184. [CrossRef]
8. Narendran, N.; Gu, Y. Life of LED-based white light sources. *J. Disp. Technol.* **2005**, *1*, 167–171. [CrossRef]
9. Chang, M.H.; Das, D.; Varde, P.V.; Pecht, M. Light emitting diodes reliability review. *Microelectron. Reliab.* **2012**, *52*, 762–782. [CrossRef]
10. Song, B.M.; Han, B.; Lee, J.H. Optimum design domain of LED-based solid state lighting considering cost, energy consumption and reliability. *Microelectron. Reliab.* **2013**, *53*, 435–442. [CrossRef]
11. Efremov, A.A.; Bochkareva, N.I.; Gorbunov, R.I.; Lavrinovich, D.A.; Rebane, Y.T.; Tarkhin, D.V.; Shreter, Y.G. Effect of the Joule heating on the quantum efficiency and choice of thermal conditions for high power blue InGaN/GaN LEDs. *Semiconductors* **2006**, *40*, 605–610. [CrossRef]
12. Huang, S.; Wu, H.; Fan, B.; Zhang, B.; Wang, G. A chip-level electrothermal-coupled design model for high-power light-emitting diodes. *J. Appl. Phys.* **2010**, *107*. [CrossRef]
13. Treurniet, T.; Lammens, V. Thermal management in color variable multi-chip LED modules. In Proceedings of the 23rd IEEE Semiconductor Thermal Measurement and Management Symposium SEMI-THERM, Dallas, TX, USA, 14–16 March 2006. [CrossRef]
14. Górecki, K.; Ptak, P. Modeling LED lamps in SPICE with thermal phenomena taken into account. *Microelectron. Reliab.* **2017**, *79*, 440–447. [CrossRef]

15. Alexeev, A.; Onushkin, G.; Linnartz, J.P.; Martin, G. Multiple heat source thermal modeling and transient analysis of LEDs. *Energies* **2019**, *12*, 1860. [CrossRef]
16. Kumar, S.K.; Wani, S.C.; Lee, R. LED thermal management of an automotive electronic control module with display. In Proceedings of the IEEE 14th Electronics Packaging Technology Conference EPTC, Singapore, 5–7 December 2012. [CrossRef]
17. Lan, K.; Moo, W.H. Thermal resistance measurement of LED package with multichips. *IEEE Trans. Compon. Packaging Technol.* **2007**, *30*, 632–636. [CrossRef]
18. Ptak, P.; Górecki, K.; Dziurdzia, B. Modelling thermal properties of large LED module. *Mater. Sci. Pol.* **2019**, *37*, 628–638. [CrossRef]
19. Wang, C.P. Effects of diode voltage and thermal resistance on the performance of multichip LED modules. *IEEE Trans. Electron Devices* **2015**, *63*, 390–393. [CrossRef]
20. Wang, C.P.; Kang, S.W.; Lin, K.M.; Chen, T.T.; Fu, H.K.; Chou, P.T. Analysis of thermal resistance characteristics of power LED module. *IEEE Trans. Electron Devices* **2013**, *61*, 105–109. [CrossRef]
21. Kim, H.; Kim, K.J.; Lee, Y. Thermal performance of smart heat sinks for cooling high power LED modules. In Proceedings of the IEEE 13th Intersociety Conference on Thermal and Thermomechanical Phenomena in Electronic Systems ITHERM, San Diego, CA, USA, 30 May–1 June 2012. [CrossRef]
22. Bahman, A.; Ma, K.; Blaabjerg, F. A lumped thermal model including thermal coupling and thermal boundary conditions for high power IGBT modules. *IEEE Trans. Power Electron.* **2017**, *33*, 2518–2530. [CrossRef]
23. Górecki, K.; Górecki, P.; Zarębski, J. Measurements of parameters of the thermal model of the IGBT module. *IEEE Trans. Instrum. Meas.* **2019**, *68*, 4864–4875. [CrossRef]
24. Deng, Z.; Zhao, Z.; Zhang, P.; Li, J.; Huang, Y. Study of the methods to measure the junction-to-case thermal resistance of IGBT modules and press pack IGBTs. *Microelectron. Reliab.* **2017**, *79*, 248–256. [CrossRef]
25. Gorecki, K. Modelling mutual thermal interactions between power LEDs in SPICE. *Microelectron. Reliab.* **2015**, *55*, 389–395. [CrossRef]
26. Ptak, P.; Górecki, K.; Wnuczko, S. Embedded system to control lighting of the office workplace. *Przegląd Elektrotechniczny* **2018**, *94*, 76–79. [CrossRef]
27. Mentor®. Available online: www.mentor.com/products/mechanical/micred/t3ster/ (accessed on 15 May 2020).
28. Szekely, V. A new evaluation method of thermal transient measurement results. *Microelectron. J.* **1997**, *28*, 277–292. [CrossRef]
29. Janicki, M.; Torzewicz, T.; Samson, A.; Raszkowski, T.; Napieralski, A. Experimental identification of LED compact thermal model element values. *Microelectron. Reliab.* **2018**, *86*, 20–26. [CrossRef]
30. JEDEC. *Implementation of the Electrical Test Method for the Measurement of Real Thermal Resistance and Impedance of Light-Emitting Diodes with Exposed Cooling Surface*; Standard JESD51-51; JEDEC: Arlington, VA, USA, 2012.
31. JEDEC. *Guidelines for Combining CIE 127-2007 Total Flux Measurement with Thermal Measurement of LEDs with Exposed Cooling Surface*; Standard JESD51-52; JEDEC: Arlington, VA, USA, 2012.
32. Janicki, M.; Torzewicz, T.; Ptak, P.; Raszkowski, T.; Samson, A.; Górecki, K. Parametric compact thermal models of power LEDs. *Energies* **2019**, *12*, 1724. [CrossRef]
33. Janicki, M.; Napieralski, A. Considerations on Electronic System Compact Thermal Models in The Form of RC Ladders. In Proceedings of the 15th International Conference the Experience of Designing and Application of CAD Systems CADSM, Polyana, Ukraine, 26 February–2 March 2019.
34. Gerstenmaier, Y.C.; Kiffe, W.; Wachutka, G. Combination of Thermal Subsystem Modeled by Rapid Circuit Transformation. In Proceedings of the 13th International Workshop on Thermal Investigation of ICs and Systems, Budapest, Hungary, 17–19 September 2007; pp. 115–120. [CrossRef]
35. Poppe, A.; Zhang, Y.; Wilson, J.; Farkas, G.; Szabo, P.; Parry, J.; Rencz, M.; Szekely, V. Thermal measurement and modeling of multi-die packages. *IEEE Trans. Compon. Packag. Technol.* **2009**, *32*, 484–491. [CrossRef]

© 2020 by the authors. Licensee MDPI, Basel, Switzerland. This article is an open access article distributed under the terms and conditions of the Creative Commons Attribution (CC BY) license (http://creativecommons.org/licenses/by/4.0/).